M. Munavar Hussain, B. H. Doreswamy, N. C. Shobha, V. N. Vijayakumar, K. Fakruddin, Orientational order parameter of liquid crystalline nanocomposites by Newton's rings and image analysis methods,
Nanosystems: Physics, Chemistry, Mathematics, 2019, Volume 10, Issue 3, 243–254

NANOSYSTEMS: PHYSICS, CHEMISTRY, MATHEMATICS, 2019, 10 (3), P. 243–254

Orientational order parameter of liquid crystalline nanocomposites by Newton's rings and image analysis methods

M. Munavar Hussain[1]*, B. H. Doreswamy[2], N. C. Shobha[3], V. N. Vijayakumar[4], K. Fakruddin[5]

[1]Department of Physics, KNS Institute of Technology, Bengaluru, India
[2]Department of Physics, SJB Institute of Technology, Bengaluru, India
[3]Department of Physics, APS College of Engineering, Bengaluru, India
[4]Department of Physics,Bannari Amman Institute of Technology, Sathyamangalam, India
[5]Department of Physics, Ghousia College of Engineering, Ramanagara, India

*munavar.phd@gmail.com

DOI 10.17586/2220-8054-2019-10-3-243-254

Liquid crystalline nanocomposites are prepared by dispersing TiO_2, ZnO, Fe_2O_3 and Fe_3O_4 nanoparticles separately in 4-Cyano 4'-Propoxy-1, 1'-Biphenyl (3O-CB) liquid crystal in a 1:100 ratio. The characteristic textures exhibited are captured at different liquid crystalline phases by using POM. The phase transition temperatures are measured by both polarizing optical microscope (POM) and differential scanning calorimeter (DSC). The optical textures are analyzed by using MATLAB software to compute birefringence and order parameter of samples. The birefringence and order parameter also measured by conventional Newton's rings technique, the results are discussed.

Keywords: liquid crystals, nanocomposites, optical textures, phase transition temperatures, birefringence, order parameter.

Received: 12 November 2018

Revised: 19 April 2019

1. Introduction

Liquid crystal technology has a major effect on many areas of science and technology. Applications of this kind of materials are being discovered and continued to provide effective solution to many different problems. For modern industrial application, wide temperature range of liquid crystal phase, high optical and dielectric anisotropy and fast switching time are required. By composing liquid crystalline mixtures or using guest materials in host liquid crystals are two basic methods for obtaining liquid crystals with enhanced properties. Metal oxide nanoparticles are novel type of guest materials. Doping nanomaterials in liquid crystals enhances the properties of liquid crystals. Different types of metal oxide nanoparticles are used to achieve this purpose [1].

Liquid crystals, being anisotropic media, provide good support for self-assembly of nanomaterials into large organizing structures in multiple dimensions. Therefore, doping of nanoparticle into liquid crystals has emerged as a fascinating area of applied research. Nano objects (Guests) are embedded in the liquid crystals (Hosts) that can trap the ion concentration, electrical conductivity and improve the electro-optical response of the host [2].

Incorporation of metal oxide nanoparticles into liquid crystals makes it easier to obtain better display parameter profiles [3]. The metal oxide nanoparticles embedded in liquid crystal bases have attracted much interest not only in the field of magnetic recording media but also in the area of medical care. The medical applications,which include radio frequency, hyperthermia, photo magnetic and magnetic resonance imaging, cancer therapy, sensors and high frequency applications, were reported [4–7].

In the present work, an effort has been made to study the effect of metal oxide nanoparticles on the orientation order parameter of 4-Cyano 4'-Propoxy-1, 1'-Biphenyl liquid crystal by image analysis and Newton's ring techniques. There are several techniques for studying the temperature dependence of liquid crystal properties [8–11]. But they involve technical difficulties in measuring required parameters.

In this paper, we have explored image analysis-computer program technique to find orientation order parameter of liquid crystalline nanocomposites. In the image analysis technique, textures of liquid crystal samples are captured from crystal to isotropic phase by using POM. The changes in textural feature as a function of temperature are useful to compute thermo-optical properties of liquid crystals. By this technique, it is possible to extract as much information as possible from the textural image by means of applying computational algorithms on image data or intensity values. MAT LAB software [12, 13] is used for the analysis of liquid crystal textures and to estimate the orientational order parameter.

TABLE 1. Liquid crystalline compound and its nanocomposites

S_l. No.	Liquid crystalline compound (100 mg)	Metal oxide nanoparticles (1 mg)	Liquid crystalline nanocomposites
1	4-Cyano 4'-Propoxy-1, 1'-Biphenyl ($C_{16}H_{15}NO$)	—	S_1
2	4-Cyano 4'-Propoxy-1, 1'-Biphenyl ($C_{16}H_{15}NO$)	ZnO	S_{11}
3	4-Cyano 4'-Propoxy-1, 1'-Biphenyl ($C_{16}H_{15}NO$)	TiO_2	S_{12}
4	4-Cyano 4'-Propoxy-1, 1'-Biphenyl ($C_{16}H_{15}NO$)	Fe_3O_4	S_{13}
5	4-Cyano 4'-Propoxy-1, 1'-Biphenyl ($C_{16}H_{15}NO$)	Fe_2O_3	S_{14}

2. Materials and methods

In this present work 4-Cyano 4'-Propoxy-1, 1'-Biphenyl liquid crystal was purchased from TCI, Ltd. and ZnO, TiO_2, Fe_3O_4 and Fe_2O_3 nanoparticles were obtained from VTU-PG centre, Muddenahalli, Chikkaballapura District, Bengaluru, India. Liquid crystalline nanocomposites are prepared using sonication method and its composition names are given in the Table 1. Textural features are studied using POM to confirm its liquid crystalline behavior. Then the transition temperature is measured with DSC studies for reliable information. Optical parameters like birefringence and order parameters of such nanocomposites are studied using conventional newton's ring method as well as computational methods using MATLAB program.

3. Results and discussions

3.1. Polarizing optical microscope

The liquid crystalline nanocomposites are characterized by different liquid crystalline phases due to the changes in local molecular order with temperature [14]. The characterization of these mesophases will provide very important information on the pattern and textures of LCs. The transition temperatures and optical textures observed by polarizing optical microscope is shown in Figs. 1–5. As a representative case, the schelieren texture of nematic phase from isotropic phase is observed at 61.5 °C then it is grown to curved brushes texture observed at 54 °C and finally at 47.5 °C the crystalline texture is formed which is not transparent hence look dark, all this textures are represented in the set of Fig. 1.

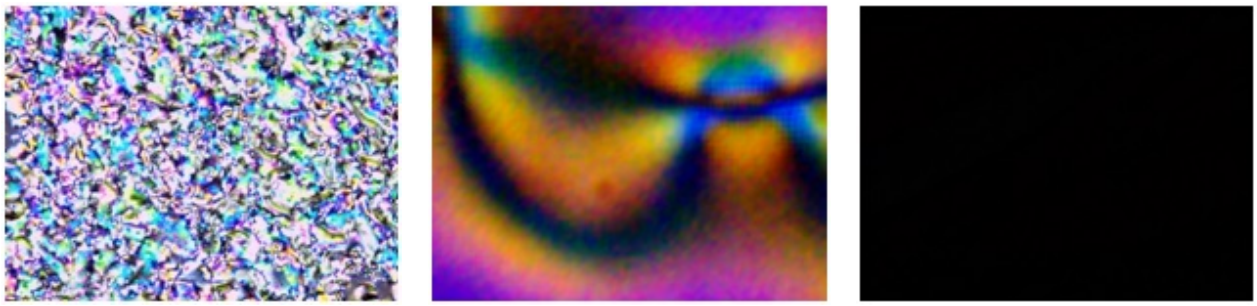

(a) (b) (c)

FIG. 1. POM Textures of sample S_1: Isotropic – Nematic Transition Phase @ 61.5 °C (a); Nematic Phase @ 54 °C (b); Solid Phase @ 47.5 °C (c)

Dispersion of nanoparticles with liquid crystal influenced the textural features of the sample at different phases with respect to temperature and nanomaterial is observed in POM textures. The surface to volume ratio of sample liquid crystal increases due to surface restructuring by nanoparticle dispersion. This phenomenon of molecular restructuring varies as a function of temperature and nanoparticle composition. It is observed that orientational order of liquid crystal molecules are further strengthened heavily at isotropic to nematic phase and strengthened less at

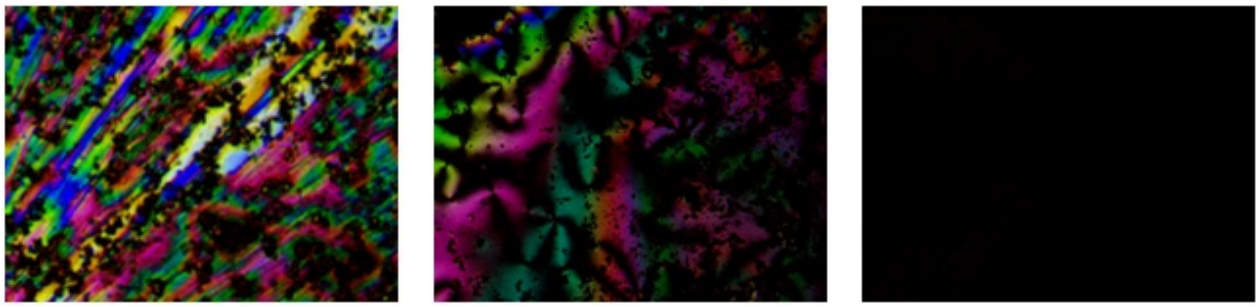

(a) (b) (c)

FIG. 2. POM Textures of sample S_{11}: Isotropic – Nematic Transition Phase @ 60.5 °C (a); Nematic Phase @ 56.5 °C (b); Solid Phase @ 46 °C (c)

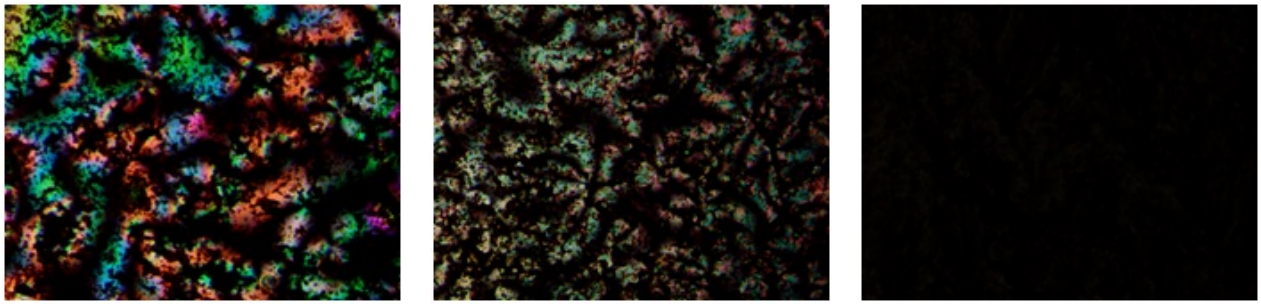

(a) (b) (c)

FIG. 3. POM Textures of sample S_{12}: Isotropic – Nematic Transition Phase @ 60.5 °C (a); Nematic Phase @ 56.5 °C (b); Solid Phase @ 46 °C (c)

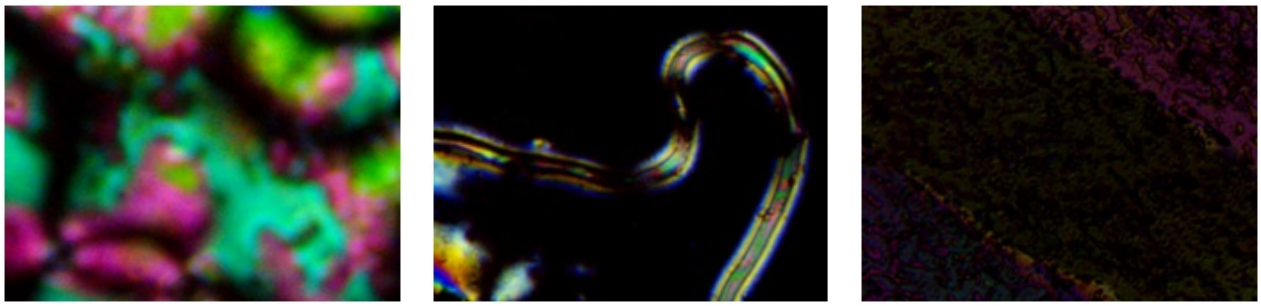

(a) (b) (c)

FIG. 4. POM Textures of sample S_{13}: Isotropic – Nematic Transition Phase @ 59.5 °C (a); Nematic Phase @ 54 °C (b); Solid Phase @ 50 °C (c)

crystalline phase by the nanoparticles with shifting transition temperature. This is because possibility of increasing its surface area and decreasing its volume. It is also observed that molecular weight of nanoparticles plays vital role in re-structuring liquid crystal molecules. The observation of POM shows that restructuring of molecules leads to defective textural images at various instances.

Phase transition temperatures observed for liquid crystalline nanocomposites using POM and DSC shows that they are reduced due to the dispersion of nanoparticles. The nanoparticles ZnO, TiO_2, Fe_3O_4 and Fe_2O_3 influences the liquid crystal and reduces the transition temperature by 1 °C, 1 °C, 1 °C and 2 °C respectively.

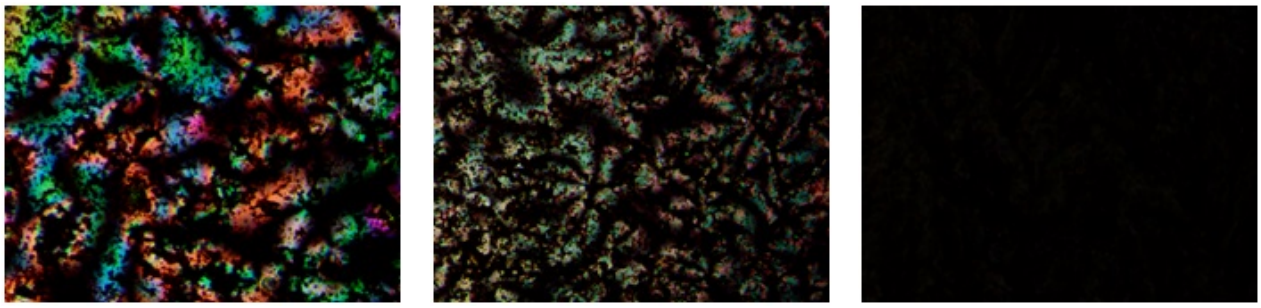

(a) (b) (c)

FIG. 5. POM Textures of sample S_{14}: Isotropic – Nematic Transition Phase @ 60.5 °C (a); Nematic Phase @ 52 °C (b); Solid Phase @ 49.5 °C (c)

3.2. Differential scanning calorimeter (DSC) studies

The thermal analysis by DSC study provides data regarding the temperatures and heat capacity of different phases. DSC study reveals presence of phase transition in materials by detecting the enthalpy change associated with each phase transition. DSC study is used in conjunction with optical polarizing microscopy to determine the mesophase types exhibited by the materials. The different thermograms of liquid crystalline nanocomposites are recorded from DSC as shown in Figs. 6, 7.

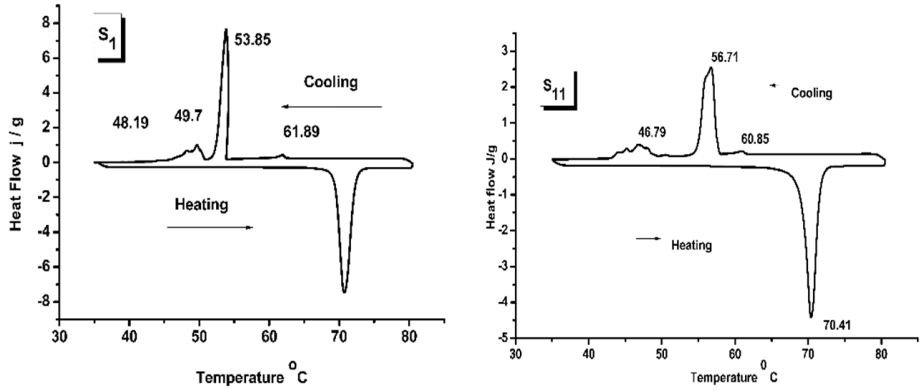

(a) (b)

FIG. 6. DSC Thermogram of sample S_1 (a) and S_{11} (b)

The phase transition temperatures obtained by POM and DSC are tabulated for pure and nanocomposites liquid crystals at different phases in Table 2. The samples show isotropic, nematic and crystalline phases. The phases of samples are confirmed with the help of POM images obtained and corresponding transition temperatures are considered with the help of DSC values. The temperatures are measured in degree centigrade (°C). The enthalpy jump at various phase is noted in the given table with in units of Joules per gram (J/g).

3.3. Birefringence studies by Newton's rings method

The experimental setup consists of plano-convex lens of small radius of curvature (13 mm) and plane glass plate which is being placed in hot stage connected to specially designed microcontroller based temperature and image capturing device. The LC sample is introduced between the glass plate and lens and set the polarizer and the analyzer in the crossed position. The hot stage along with LC sample mount is placed on the microscope stage and then adjust hot stage axis to coincide with the microscopic axis. Set the reflector of the microscope to pass the light through LC sample until the clear Newton's rings are formed on the monitor. These rings are formed due to the interference of ordinary and extra ordinary rays after passing through the analyzer. The diameter of various rings was measured. The experimental setup is shown in the Fig. 8 and ring pattern in Fig. 9.

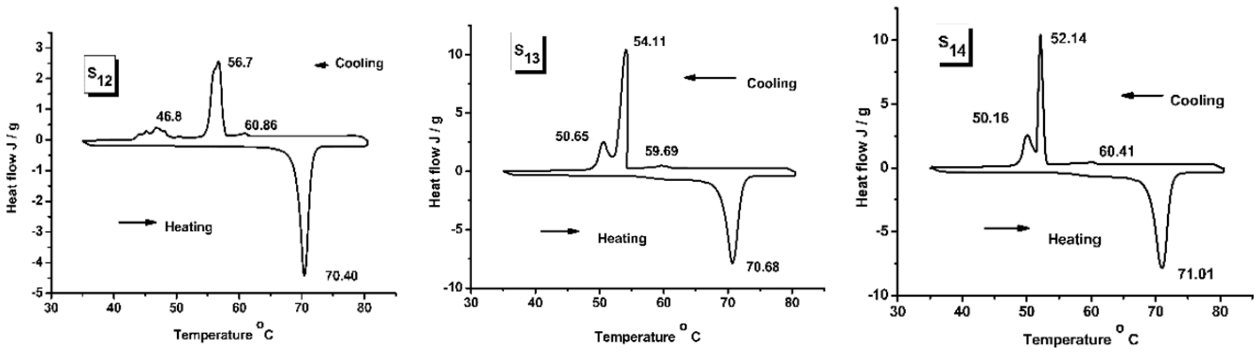

(a) (b) (c)

FIG. 7. DSC Thermogram of sample S_{12} (a), S_{13} (b) and S_{14} (c)

TABLE 2. Phase transition temperature of S_1, S_{11}, S_{12}, S_{13} and S_{14}

Nano Composite LC	Study	Unit	Phase Variance		
			I–N	N	N-Crystal state
S_1	POM	°C	62	52	
	DSC	°C J/g	61.89 (0.22)	53.85 (7.23)	49.7 (30.11)
S_{11}	POM	°C	61.21	56.98	
	DSC	°C J/g	60.85 (0.24)	56.71 (6.32)	46.79 (13.54)
S_{12}	POM	°C	61.41	57.2	
	DSC	°C J/g	60.86 (0.26)	56.7 (6.51)	46.8 (14.22)
S_{13}	POM	°C	60.32	55	
	DSC	°C J/g	59.69 (0.78)	54.11 (8.79)	50.65 (31.15)
S_{14}	POM	°C	61.23	53.17	
	DSC	°C J/g	60.41 (0.86)	52.14 (8.14)	50.16 (30.55)

The optical path difference between e-ray (extra ordinary ray) and o-ray (ordinary ray) is given by y, δn which corresponds to ring number k and wavelength λ for a bright fringe is given by:

$$\delta n = \frac{k\lambda}{y}, \tag{1}$$

$$y = \frac{x^2}{2R}. \tag{2}$$

From equations (1) and (2):

$$\delta n = (2R\lambda)\frac{k}{x^2}. \tag{3}$$

Since $2R\lambda = c$, cell constant for the given wavelength of light:

$$\delta n = \frac{ck}{x^2}, \tag{4}$$

where x is the radius of the ring and R – the radius of curvature of the lens used.

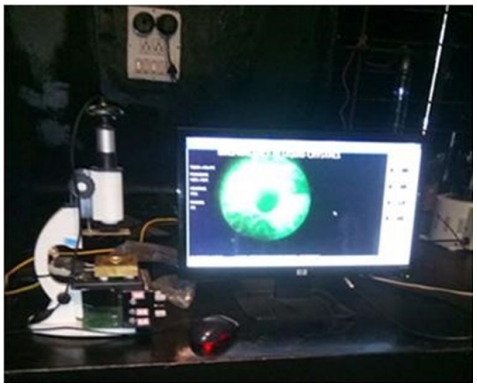

FIG. 8. Experimental setup to measure birefringence (Newtons rings method)

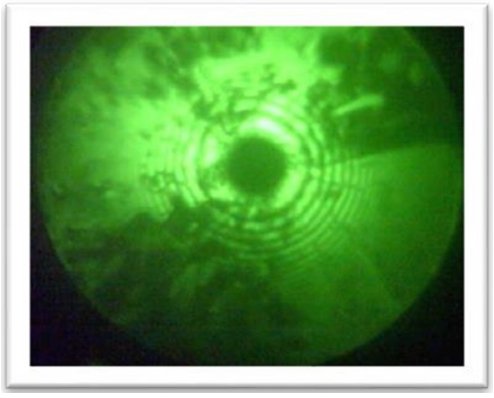

FIG. 9. Newtons Rings observed in samples S_1 at temperatures 59 °C

δn can be measured with great accuracy by finding the slope of the straight line drawn between x^2 versus the ring number k and shown in Figs. 10–12. We can obtain the same result by considering the dark rings also. The schematic diagram is shown in Fig. 13.

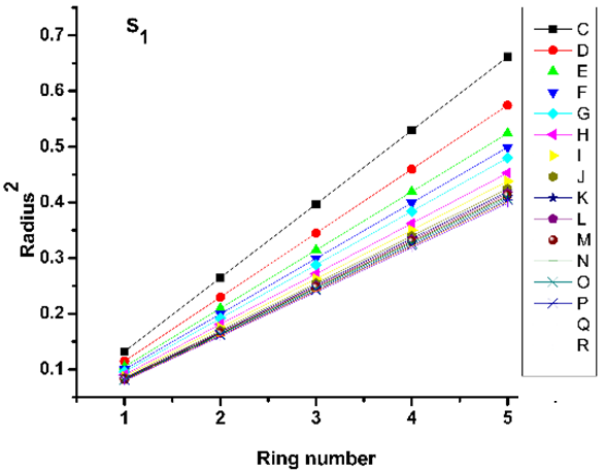

FIG. 10. The square of radius of ring Vs ring number at various temperature of sample S_1

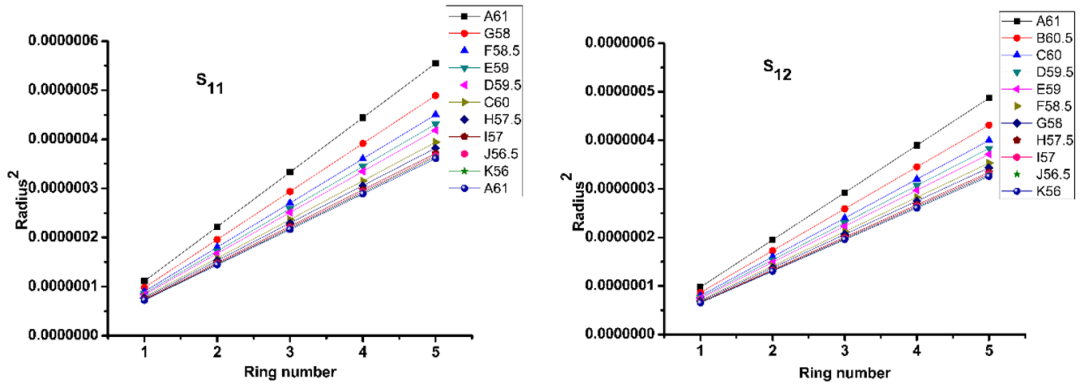

(a) (b)

FIG. 11. The square of radius of ring Vs ring number at various temperature of sample S_{11} (a) & S_{12} (b)

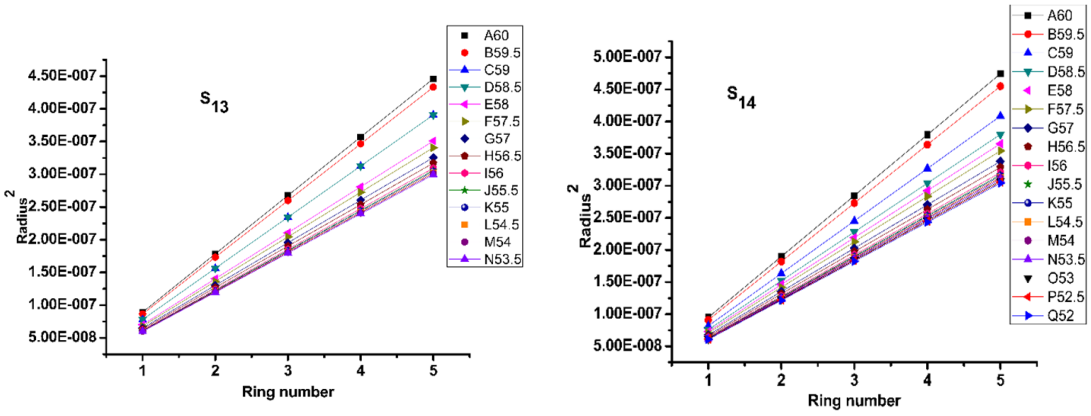

(a) (b)

FIG. 12. The square of radius of ring Vs ring number at various temperature of sample S_{13} (a) & S_{14} (b)

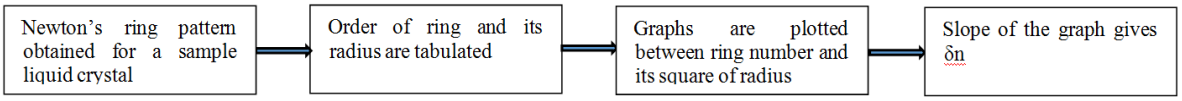

FIG. 13. Schematic diagram of Newtons Rings method for calculation of birefringence (δn)

As the temperature decreases, birefringence δn increases. The method adopted for the estimation of orientational order parameter from δn given by Kuczynski et al. as follows where Δn is birefringence at crystalline phase and is obtained by linear regression method shown in Figs. 14–16 [15, 16]:

$$S = \frac{\delta n}{\Delta n}. \tag{5}$$

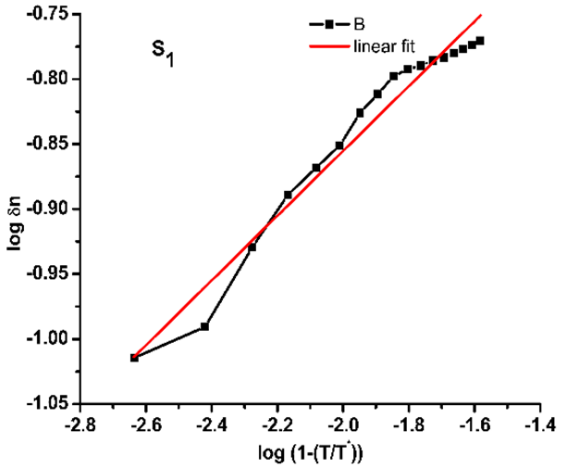

FIG. 14. $\log \delta n$ and $\log(1-(T/T^*))$ graph of S_1 by Newtons rings method

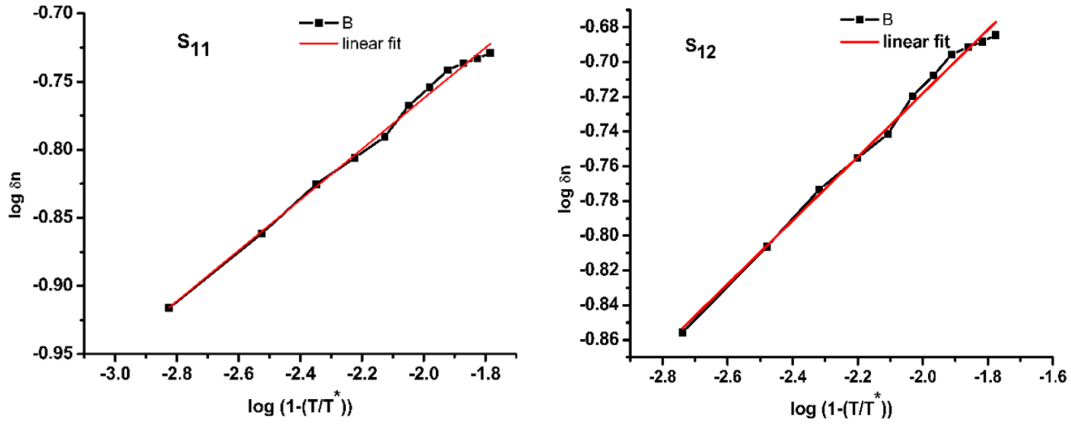

(a) (b)

FIG. 15. $\log \delta n$ and $\log(1-(T/T^*))$ graph of S_{11} (a) and S_{12} (b) by Newtons rings method

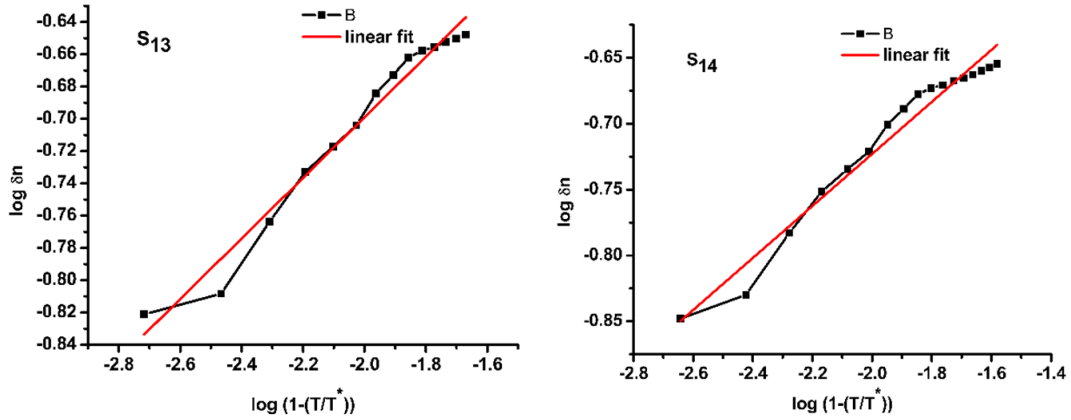

(a) (b)

FIG. 16. $\log \delta n$ and $\log(1-(T/T^*))$ graph of S_{13} (a) and S_{14} (b) by Newtons rings method

3.4. Birefringence and order parameter by image analysis

Phase transitions are characterized by abrupt changes, discontinuities, breaking of symmetry and strong fluctuations of the molecules in a compound. The identification of transition temperatures is essential to study the physical properties of the LC materials. The transition also indicates the transformation from an ordered phase to relatively disordered phase and Vice versa as the temperatures are raised or cooled [17, 18].

The behavior of light with respect to temperature is known as the thermo-optical parameters. Optical birefringence and order parameters are the important thermo-optical parameters. Image analysis is the extraction of meaningful information from images (Textures) by applying computational techniques and algorithms to image data. Image analysis technique compute the statistics and measurement based on grey level intensities of the image pixels. In the present work, optical birefringence and order parameter are computed from the optical textures of samples as a function of temperatures by image analysis technique.

The birefringence of the liquid crystals was measured as a function of temperature by substituting the thickness d of liquid crystalline sample layer and wavelength of color in the following equation to calculate birefringence [8]:

$$I = I_0 \sin^2\left(\frac{\pi d \delta n}{\lambda}\right), \tag{6}$$

where d is thickness of liquid crystal layer, I_0 is the intensity of light observed when there is no sample (Liquid crystal layer) between light source and lens, I is the Intensity of light observed when there is sample (Liquid crystal layer).

The temperature dependent birefringence values of the samples are used to calculate the order parameter using Kuczynski equation given below [16, 19]:

$$S = \frac{\delta n}{\Delta n}, \tag{7}$$

where Δn is birefringence at crystalline stateand is obtained by linear regression method using Newton's rings experiment.

In the image analysis technique, optical textures, thickness of the liquid crystal layer (d) and birefringence in perfect order (Δn) are given as input to obtain birefringence and order parameter. The birefringence and order parameter evaluated at different liquid crystalline phases by image analysis and Newton's rings methods are represented in Tables 3–7. The order parameter values are found to be same using both methods. The order parameter found to decrease with increase of temperature. The temperature variation of order parameter is depicted in Fig. 17.

TABLE 3. Birefringence and order parameter of sample S_1 by Newton's ring and image processing methods at various phases

$\Delta n = 0.35$							$\beta = 0.24$
Temp (°C)	T (K)	Phase Variance	Newton's ring method		Image processing method		
			δn	$S = \frac{\delta n}{\Delta n}$	Thickness of sample layer (d) in meter	δn	$S = \frac{\delta n}{\Delta n}$
61.5	334.5	I–N	0.09671	0.276314286	1.12E-6	0.0957982	0.273709
54	327	N	0.1684	0.481142857	1.01E-6	0.170262	0.486463
47.5	320.5	Cr	—	—	0.81E-6	0.307646	0.878989

TABLE 4. Birefringence and order parameter of sample S_{11} by Newton's ring and image processing methods at various phases

$\Delta n = 0.391$							$\beta = 0.186$
Temp (°C)	T (K)	Phase Variance	Newton's ring method		Image processing method		
			δn	$S = \frac{\delta n}{\Delta n}$	Thickness of sample layer (d) in meter	δn	$S = \frac{\delta n}{\Delta n}$
60.5	333.5	I–N	0.13758	0.351867	1.45E-06	0.124618	0.318717
56.5	329.5	N	0.18492	0.472941	1.18E-06	0.185199	0.473655
46	319	Cr	—	—	0.72E-06	0.352115	0.90055

From our investigation it is observed that order parameter increases due to the dispersion of metal oxide nanoparticles in 4-Cyano 4'-Propoxy-1, 1'-Biphenyl liquid crystal. The percentage of increase of order parameter in nematic phase is 1.27 % to 4.5 %, 7.13 % to 15.81 %, 19.93 % to 23.1 % and 18.51 % to 19.03 % due the dispersion of ZnO, TiO_2, Fe_3O_4 and Fe_2O_3 nanoparticles respectively.

TABLE 5. Birefringence and order parameter of sample S_{12} by Newton's ring and image processing methods at various phases

$\Delta n = 0.347$							$\beta = 0.186$
Temp (°C)	T (K)	Phase Variance	Newton's ring method		Image processing method		
			δn	$S = \frac{\delta n}{\Delta n}$	Thickness of sample layer (d) in meter	δn	$S = \frac{\delta n}{\Delta n}$
60.5	333.5	I–N	0.15611	0.449885	1.30E-06	0.15156	0.431796
56.5	329.5	N	0.20503	0.590865	1.05E-06	0.195764	0.557733
46	319	Cr	—	—	0.79E-6	0.311774	0.888244

TABLE 6. Birefringence and order parameter of sample S_{13} Newton's ring and image processing methods at various phases

$\Delta n = 0.324$							$\beta = 0.188$
Temp (°C)	T (K)	Phase Variance	Newton's ring method		Image processing method		
			δn	$S = \frac{\delta n}{\Delta n}$	Thickness of sample layer (d) in meter	δn	$S = \frac{\delta n}{\Delta n}$
59.5	332.5	I–N	0.15548	0.479877	1.00E-06	0.163524	0.504705
54	327	N	0.22365	0.690278	9.70E-07	0.222162	0.685685
50	323	Cr	—-	—-	0.788E-6	0.291083	0.898404

TABLE 7. Birefringence and order parameter of sample S_{14} by Newton's ring and image processing methods at various phases

$\Delta n = 0.329$							$\beta = 0.197$
Temp (°C)	T (K)	Phase Variance	Newton's ring method		Image processing method		
			δn	$S = \frac{\delta n}{\Delta n}$	Thickness of sample layer (d) in meter	δn	$S = \frac{\delta n}{\Delta n}$
60	333	I–N	0.141953	0.431468	1.1E-06	0.152654	0.463995
52	325	N	0.221508	0.673277	1.02E-06	0.220937	0.671541
49.5	322.5	Cr	—	—	0.78E-6	0.295959	0.899572

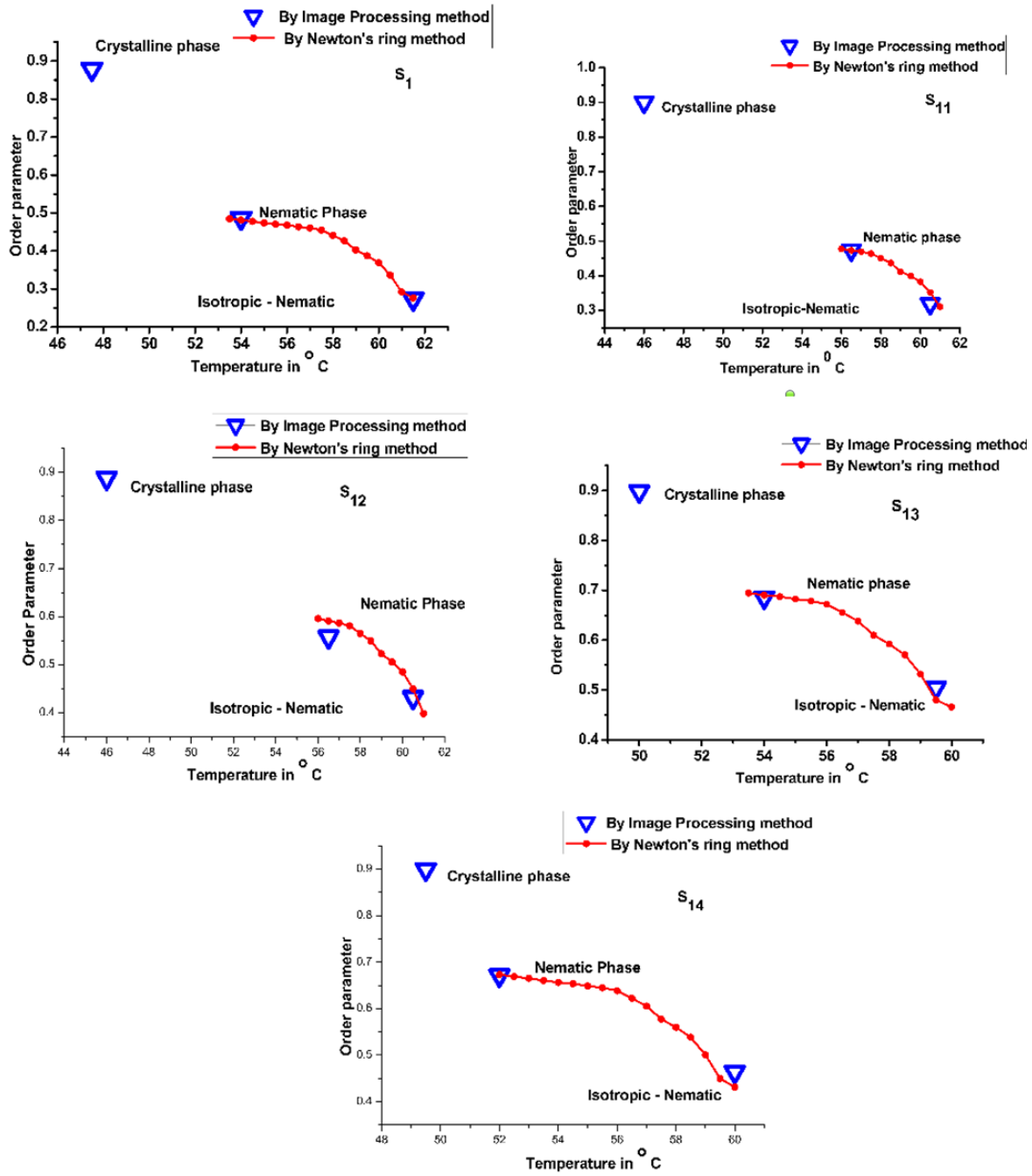

FIG. 17. Order parameter with respect to temperature by Newtons rings method and Image analysis method in samples S_1, S_{11}, S_{12}, S_{13} and S_{14}

4. Conclusion

The advantage of the image analysis method is that it is simple, less complex, efficient and reliable in this type of studies, unlike other techniques, there is no need to arrange different experimental setup except to arrange POM. By conventional techniques, the order parameter can be estimated in the nematic and smectic phases only; however, in the image analysis method, the order parameter can be evaluated in the crystalline phase in addition to the nematic and smectic phases. By the image analysis technique, the order parameter can be estimated in all liquid crystalline phases such as nematic, smectic and crystalline phases, whereas in Newton's rings method it can be evaluated only in nematic, smectic phases. Due to the dispersion of Nano particles, the birefringence anisotropy increases. Therefore,the view angle increases and this can be most advantageous in liquid crystal display devices, to produce large panel LC displays with good depth.

Acknowledgements

The authors are very much thankful to the management of Ghousia College of Engineering, Ramanagara, India and Bannari Amman Institute of Technology, Sathyamangalam, India for providing lab facilities to carry out this work. The authors also thankful to Dr. Dinesh Rangappa, VTU-PG centre, Muddenahalli, chikkaballapura Dist, Bengaluru, India for sponsoring nanoparticles.

References

[1] Kobayashi S., Miyama T., et al. Dielectric Spectroscopy of Metal Nanoparticle Doped Liquid Crystal Displays Exhibiting Frequency Modulation Response. *J. Display Technology*, 2006, **2**, P. 121–129.

[2] Garbovskiy Y., Glushchenko I. Nano-Objects and Ions in Liquid Crystals: Ion Trapping Effect and Related Phenomena. *Crystals*, 2015, **5** (4), P. 501–533.

[3] Goel P. Arora M., Biradar A.M. Electro-optic switching in iron oxide nanoparticle embedded paramagnetic chiral liquid crystal via magneto-electric coupling. *Journal of Applied Physics*, 2014, **115** (12), P. 124905(1–6).

[4] Silva J.B., deBrito W., Mohallem N.D.S. Influence of heat treatment on cobalt ferrite ceramic powders. *Materials Science and Engineering: B*, 2004, **112** (2–3), P. 182–187.

[5] Sun S., Murray C.B., et al. Monodisperse FePt nanoparticles and ferromagnetic FePt nanocrystal super lattices. *Science*, 2000, **287** (5460), P. 1989–92.

[6] Pankhurst Q.A., Connolly J., Jones S.K., Dobson J. Applications of magnetic nanoparticles in biomedicine. *Journal of Physics D: Applied Physics*, 2003, **36**, P. R167–R181.

[7] Ito A., Shinkai M., Honda H., Kobayashi T. Medical application of functionalized magnetic nanoparticles. *J. BiosciBioeng*, 2005, **100** (1), P. 1–11.

[8] Avci N., Nesrullajev A., Oktik S. Nonlinear thermotropic and thermo- optical behaviour of planar oriented textures in nematic liquid crystals at phase transitions. *Brazilian Journal of Physics*, 2010, **40**, P. 224–227.

[9] Shin-Tson Wu, Uzi Efron, LaVerne D. Hess. Birefringence measurements of liquid crystals. *Applied Optics*, 1984, **23** (21), P. 3911–3915.

[10] Fakruddin K., Jeevan Kumar R., Datta Prasad P.V., Pisipati V.G.K.M. Orientational Order Parameter – 1 A Birefringence Study. *Molecular Crystals and Liquid Crystals*, 2009, **511**, P. 133–146.

[11] Pardhasaradhi P., Datta Prasad P.V., et al. Orientational order parameter studies in two symmetric dimeric liquid crystals – an optical study. *Phase Transitions*, 2012, **85** (12), P. 1031–1044.

[12] Gonzalez R.C., Woods R.E., Eddins S.L. *Digital Image Processing Using MATLAB*, 2nd Edition, Gates mark Publishing, Natick, 2009.

[13] Solomon C., Breckon T. *Fundamentals of Digital Image Processing: A Practical Approach with Examples in Matlab*, Wiley-Blackwell, Chichester, U.K., 2011.

[14] Priestley E.L., Wojtowicz P.J., Sheng P. *Introduction to Liquid Crystals*, RCA Laboratories, Princeton, NJ, 1974.

[15] Kuczynski W., Zywucki B., Malecki J. Determination of orientational order parameter in various liquid-crystalline phases. *Mol. Cryst. Liq. Cryst.*, 2002, **381**, P. 1–19.

[16] Zywicki B.J., Kuczynski W. IEEE transactions on optical phenomena – The orientational order in nematic liquid crystals from birefringence measurements. *Dielectr. Electr. Insul.*, 2001, **8**, P. 512–515.

[17] Chandra Sekhar S. *Liquid Crystals*, Cambridge University Press: New York, 1992.

[18] Singh S. Phase transitions in liquid crystals. *Phys. Rep.*, 2000, **324**, P. 107–269.

[19] De Jeu W.H. *Physical Properties of Liquid Crystalline Materials*, Gordon and Breach, New York, 1980.